Biochemical and Biophysical Research Communications 423 (2012) 863–866

Contents lists available at SciVerse ScienceDirect

Biochemical and Biophysical Research Communications

journal homepage: www.elsevier.com/locate/ybbrc

Resolving the spatial kinetics of electric pulse-induced ion release

Hope T. Beier [a,*], Caleb C. Roth [b], Gleb P. Tolstykh [a], Bennett L. Ibey [a]

[a] Air Force Research Laboratory, 4141 Petroleum Road, Fort Sam Houston, TX 78234, USA
[b] General Dynamics Information Technology, 4141 Petroleum Road, Fort Sam Houston, TX, USA

ARTICLE INFO

Article history:
Received 7 June 2012
Available online 17 June 2012

Keywords:
Pulsed electric field
Nanosecond electric pulse
Fluorescence imaging
Calcium
Nanopores

ABSTRACT

Exposure of cells to nanosecond pulsed electric fields (nsPEF) causes a rapid increase in intracellular calcium. The mechanism(s) responsible for this calcium burst remains unknown, but is hypothesized to be from direct influx through nanopores, the activation of specific ion channels, or direct disruption of organelles. It is likely, however, that several mechanisms are involved/activated, thereby resulting in a complex chain of events that are difficult to separate by slow imaging methods. In this letter, we describe a novel high-speed imaging system capable of determining the spatial location of calcium bursts within a single cell following nsPEF exposure. Preliminary data in rodent neuroblastoma cells are presented, demonstrating the ability of this system to track the location of calcium bursts *in vitro* within milliseconds of exposure. These data reveal that calcium ions enter the cell from the plasma membrane regions closest to the electrodes (poles), and that intracellular calcium release occurs in the absence of extracellular calcium. We believe that this novel technique will allow us to temporally and spatially separate various nsPEF-induced effects, leading to powerful insights into the mechanism(s) of interaction between electric fields and cellular membranes.

© 2012 Elsevier Inc. All rights reserved.

1. Introduction

Elevation in intracellular calcium is known to occur within seconds after exposure to nanosecond pulsed electric fields (nsPEF) [1–7]. Seminal observations demonstrating this phenomenon, along with a lack of propidium iodide uptake, prompted a hypothesis that direct poration of organelles within the cell is occuring. This idea was supported by electric circuit-based models of the cell as a two-compartment system (plasma and nuclear membrane), which predicted a higher intracellular potential for nsPEF than for longer pulses classically used in electroporation [2,3]. Multiple studies have empirically suggested that intracellular membranes/organelles are being affected by nsPEF exposure [8–10].

Vernier et al. demonstrated plasma membrane disruption and calcium uptake for very short pulses, suggesting that the plasma membrane is not sparred by the field, but rather small, propidium-impermeable nanopores, penetrable by small ions, are formed [11–14]. This hypothesis was further supported by Pakhomov et al. who showed very fast cellular uptake of thallium ions following nsPEF, despite the cells being bathed in a channel-blocking buffer to inhibit passage of thallium ions through channels [15]. The existence of nanopores as both a naturally occurring membrane disruption and following nsPEF has been further confirmed by a variety of measurement techniques [16–18].

Craviso et al. concluded, through a series of experiments using specific channel blockers, that calcium uptake is regulated by L-type calcium channels and that activation of these channels is mediated by an influx of sodium ions [19,20]. The source of the sodium ions remains unknown, but may result from direct channel activation or through nanopores formed within the plasma membrane.

Consequently, it remains unclear whether calcium ions enter the cell through nanopores, ion channels, or are released from intracellular stores. Due to the highly reactive nature of calcium and calcium-dependent chemical pathways within cells, it is likely that several mechanisms occur, resulting in a compound series of events. Calcium release has thus far been monitored as a change in whole-cell fluorescence through conventional imaging methods, such as epi-fluorescence and confocal microscopy, which are too slow to capture the nearly instantaneous steps likely involved in nsPEF-induced calcium influx. Additionally, due to signal-to-noise constraints, little or no spatial information can be gathered at high rates (<1 fps). By monitoring the spatial kinetics of calcium in high-speed, we believe insights into the mechanism(s) responsible for the increase in intracellular calcium following nsPEF can be gained. In this letter, we demonstrate the capability of our high-speed fluorescence imaging system and detail preliminary data supporting this claim.

* Corresponding author. Fax: +1 210 539 7690.
E-mail address: hopebeier@gmail.com (H.T. Beier).

0006-291X/$ - see front matter © 2012 Elsevier Inc. All rights reserved.
http://dx.doi.org/10.1016/j.bbrc.2012.06.055

2. Material and methods

To image calcium release into cells at high speed, rodent neuroblastoma cells (NG108-15, ATCC) were cultured according to ATCC protocol and allowed to adhere to a glass-bottom poly-L-lysine coated 35 mm culture dish for 24 h. A standard loading buffer solution consisting of 2 mM $MgCl_2$, 5 mM KCL, 10 mM HEPES, 10 mM Glucose, 2 mM $CaCl_2$, and 135 mM NaCl was created with a pH of 7.4 and osmolarity of 290–310 mOsm. To load the cells, 2 μL of 3 mM Calcium Green 1 AM ester (CaGr) was added to 2 mL of loading buffer and incubated at 37 °C for 30 min. After 30 min of loading, the loading buffer was removed and 2 mL of exposure buffer was added to the culture dish. The exposure buffers used in this letter were either complete loading buffer, loading buffer without $CaCl_2$ and with 2 mM K-EGTA (to chelate any residual calcium), or loading buffer without $CaCl_2$, with K-EGTA, and 1 μM Thapsagargin (to deplete intracellular calcium stores). The cells were allowed to incubate in the exposure buffer for 30 min prior to nsPEF exposure to avoid stress induced by changes in buffer solution.

Excitation of the intracellular fluorescent dye was accomplished with an Argon-Krypton ion laser, tuned to 488 nm. This specific laser was chosen for its tunability across the visible spectrum to properly excite most commercially available fluorescent dyes. The beam was routed through a variable beam expander to allow for adjustable illumination diameters of 40–150 μm at the sample plane. The laser beam was then coupled through the epi-illumination pathway of an inverted microscope (Olympus X51) and through a 100× (1.4 NA, oil) objective. Fluorescence emission was collected by the same objective and after filtering (Semrock), delivered to an EM-CCD camera (Andor iXon3 897). The addition of an adjustable region-of-interest cropping and binning allow us to acquire images at a speed of ~1 ms/frame. The irradiance at the cell plane was limited to 10 W/cm^2 and cells were only exposed during the acquisition period by using an electronic beam shutter. This precaution was introduced to limit photobleaching and phototoxicity within the sample.

NsPEFs with 600-ns pulsewidth and applied voltages of 500 V were delivered to an individual cell by a custom-built micro-electrode probe that consists of two 125-μm diameter tungsten wires positioned in parallel with a gap spacing of ~100 μm. To expose a single cell, the electrodes were positioned 50 μm above the glass surface using a micromanipulator (Sutter), as show in Fig. 1. An FDTD model of the electrode geometry predicted an E-field of roughly 16.2 kV/cm at the cell. Timing of the imaging system, laser irradiation, and nsPEF delivery was controlled using a digital delay generator (Stanford Research Systems). This enabled very precise timing of the experiment with jitters measured to be only 4 ns for the pulser and ~1 μs for the camera. Accurate delivery of the pulse was monitored on a 500-MHz oscilloscope for each pulse using a high voltage probe across a load-matching resistor placed in parallel across the electrodes.

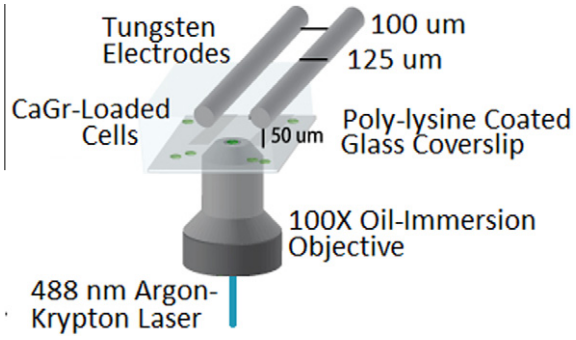

Fig. 1. Diagram of CaGr loaded cell with the custom nsPEF electrodes. The probe consists of two 125-μm diameter tungsten wires with a gap spacing of ~100 μm and are positioned 50 μm above the glass surface.

Images were processed in MATLAB. After smoothing with a mean filter with a radius of one pixel, the normalized change in fluorescence intensity, ΔF/F, was determined for each pixel, using the average of the 10 frames recorded prior to the nsPEF as the baseline. The images were then rescaled as a set. The percent change at each time was also summed vertically to provide a profile of the fluorescence change across the cell as function of time.

3. Results and discussion

The high speed calcium kinetics for nsPEF-exposed NG108 cells is shown in Fig. 2. The top image series displays the cellular response to nsPEF in the presence of extracellular calcium (Fig 2a). Within only 3.5 ms an increase in fluorescence from the cathodic side (electrodes are on the right and left of the cell) is visible. This outside-in movement of calcium is visible with progression of time. When calcium is removed from the outside solution, rather than a clear movement of calcium from the membrane inward, we observe calcium signals originating from the internal structure of the cell (Fig 2b). Interestingly, there does not appear to be a substantial time delay between cells in a calcium-rich or calcium-depleted environment. The final image series is a specific example where large vesicles were present within the cell and in the absence of extracellular calcium, an intense signal emanated from these vesicles suggesting they may have been a source of intracellular calcium release (Fig 2c). This response is of specific interest as it parallels previous observations of vesicle disruption upon nsPEF [21].

Our ability to obtain both spatial and temporal kinetics of ion release in cells is further represented in a streak-type image, which demonstrates the compound spatial response on the x-axis and time on the y-axis (Fig 3). In these images, the total intensity at each time-point is summed vertically across the middle third of the cell to provide a quantitative measure to directly compare different exposure conditions. The results are displayed as percent increase in fluorescence intensity. Image 3A corresponds to the images presented in Fig. 2a, where the cell was bathed in buffer rich in outside calcium. This temporal profile confirms the observation that, with calcium in the outside solution, there is a fast influx of calcium from the sides of the cell closest to the electrodes. However, when calcium was removed from the external solution (Fig 3B), a much lower calcium response (a max of 10% increase compared to >30%) is seen that emanates from an internal portion of the cell, possibly the endoplasmic reticulum or calcium-rich vesicle. In Fig. 3C, where calcium was again removed from the external solution, calcium emanates from multiple regions in the cell but is again diminished, as compared to Fig. 3A. In Fig. 3D, calcium has also been removed from the external solution and thapsigarin is added to deplete intra-cellular calcium stores. Here no increase in fluorescence is observed. The average whole cell fluorescence change for six cells is presented in 3e for each scenario with the shaded area representing the standard error. This difference in calcium response for the calcium-rich versus no calcium is easily seen, as well as the thapsigarin response, which closely resembles the sham exposure.

In summary, we have built a novel imaging system that opens a new avenue into the study of electromagnetic field interaction with cells. The power of this approach lies in the ability to capture both high-speed and high-resolution cellular images shortly after exposure. The data presented in this letter are exciting as they begin to decouple the mechanism(s) behind calcium uptake by cells

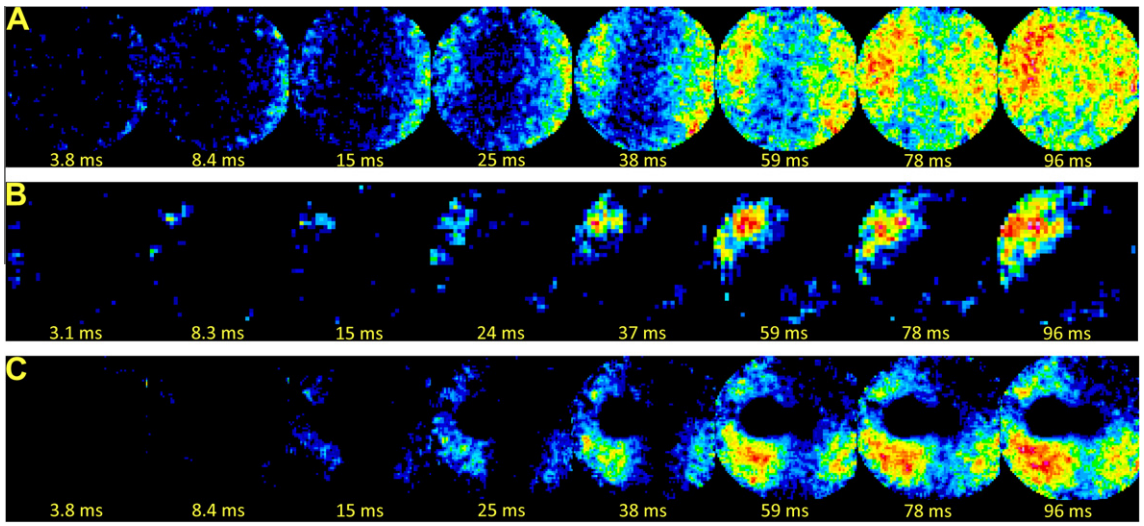

Fig. 2. Images demonstrating the temporal and spatial kinetics of calcium release into a NG108 cell after exposure to an electrical pulse. Intensity in these images is the relative ΔF/F in CaGr, which is indicative of an increase in calcium concentration. In (A), the exposed cell is bathed in a buffer rich in calcium and the influx of calcium from the electrode sides of the cell can clearly be seen. In (B), the calcium has been removed from the external buffer and the fluorescence increase is mostly confined to a localized region within the cell. In (C), the external calcium has been removed, but calcium is shown to originate from two large, internal vesicles at the sides closest to the electrodes and propagate toward the outside of the cell. The position of the electrodes is indicated with the cathode to the right and anode to the left.

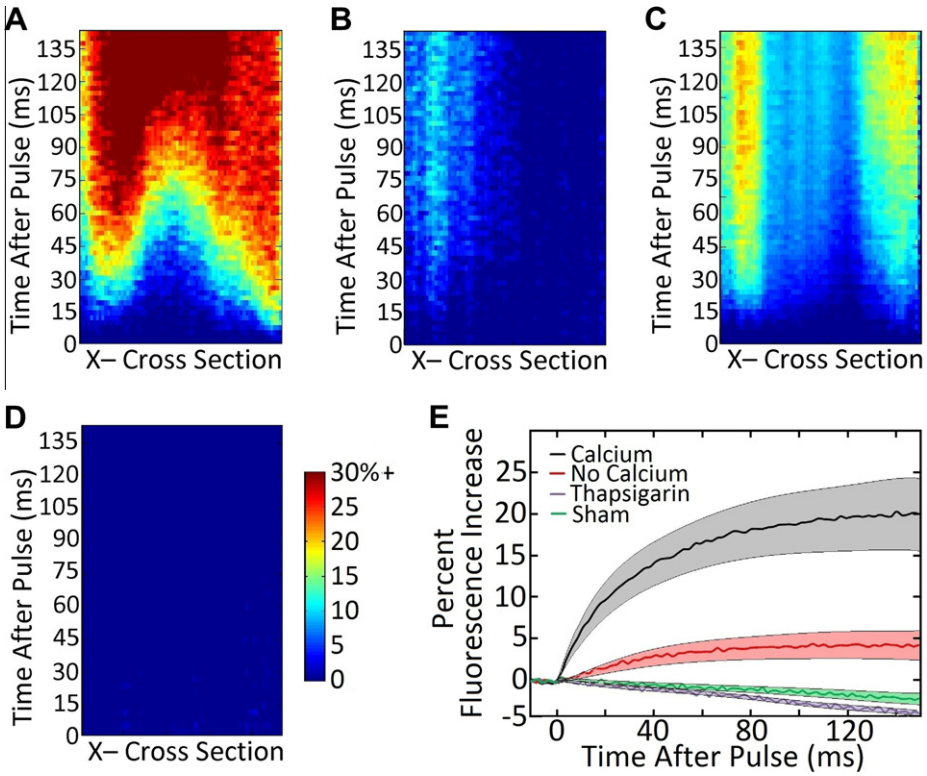

Fig. 3. Streak-type images demonstrate the compound spatial response on the x-axis versus time for various exposure conditions. In Ca^{2+}-rich buffer, (A), influx in Ca^{2+} is from the outside. With no external Ca^{2+}, (B and C), the signal is diminished and originates from local spatial region. When thapsigarin is added to deplete intra-cellular calcium stores, (D), no increase in fluorescence is observed. These results are further summarized and compared to sham exposure in (E).

following nsPEF. Specifically, external calcium enters the cell from the locations receiving the most field (poles facing the electrodes), which matches previous observations illustrating a polar-dependence on membrane-conformation changes [12], membrane depolarization [22], and propidium iodide uptake [5,6]. Such dependence agrees well with recent numerical models of pore formation [23]. Additionally, in the absence of calcium, this spatial dependence is lost and a much weaker intracellular response is observed, suggesting that nsPEF stimulation causes the release of intracellular calcium stores. Future experiments will help identify the function of sodium in this reaction by using our approach to monitor sodium uptake in cells and identify the effect of specific channel blocking agents on observed spatial and temporal response.

Acknowledgments

HTB and GPT acknowledge support of National Research Council Research Associateship Awards. HTB and BLI acknowledge support of Air Force Office of Scientific Research (AFOSR) LRIR grants #12RH01COR (Beier) and #09RH09COR (Ibey). The authors thank Shu Xiao for providing the pulsing system.

References

[1] P.T. Vernier, Y. Sun, L. Marcu, S. Salem, C.M. Craft, M.A. Gundersen, Calcium bursts induced by nanosecond electric pulses, Biochem. Biophys. Res. Commun. 310 (2003) 286–295.
[2] K.S. Schoenbach, B. Hargrave, R.P. Joshi, J. Kolb, C. Osgood, R. Nuccitelli, A.G. Pakhomov, J. Swanson, M. Stacey, J.A. White, S. Xiao, J. Zhang, S.J. Beebe, P.F. Blackmore, E.S. Buescher, Bioelectric effects of nanosecond pulses, IEEE Trans. Dielectr. Electr. Insul. 14 (2007) 1088–1109.
[3] K.H. Schoenbach, S.J. Beebe, E.S. Buescher, Intracellular effect of ultrashort electrical pulses, Bioelectromagnetics 22 (2001) 440–448.
[4] J.A. White, P.F. Blackmore, K.H. Schoenbach, S.J. Beebe, Stimulation of capacitative calcium entry in HL-60 cells by nanosecond pulsed electric fields, J. Biol. Chem. 279 (2004) 22964–22972.
[5] Y. Sun, P.T. Vernier, M. Behrend, J. Wang, M.M. Thu, M. Gundersen, L. Marcu, Fluorescence microscopy imaging of electroperturbation in mammalian cells, J. Biomed. Opt. 11 (2006) 024010–024018.
[6] P.T. Vernier, Y. Sun, L. Marcu, C.M. Craft, M.A. Gundersen, Nanosecond pulsed electric fields perturb membrane phospholipids in T lymphoblasts, FEBS Lett. 572 (2004) 103–108.
[7] J. Deng, K.H. Schoenbach, E.S. Buescher, P.S. Hair, P.M. Fox, S.J. Beebe, The effects of intense submicrosecond electrical pulses on cells, Biophys. J. 84 (2003) 2709–2714.
[8] T.B. Napotnik, Y.H. Wu, M.A. Gundersen, D. Miklavčič, P.T. Vernier, Nanosecond electric pulses cause mitochondrial membrane permeabilization in Jurkat cells, Bioelectromagnetics 33 (2012) 257–264.
[9] T.B. Napotnik, M. Rebersek, T. Kotnik, E. Lebrasseur, G. Cabodevila, D. Miklavčič, Electro-permeabilization of endocytotic vesicles in B16 F1 mouse melanoma cells, Med. Biol. Eng. Comput. 48 (2010) 407–413.
[10] Y.-H. Wu, T. Batista-Napotnik, M.A. Gundersen, D. Miklavcic, P.T. Vernier, Intracellular effects of nanosecond, high field electrical pulses, Biophys. J. 98 (2009) 404a.
[11] P.T. Vernier, M.J. Ziegler, Y. Sun, W.V. Chang, M.A. Gundersen, D.P. Tieleman, Nanopore formation and PHOSPHATIDYLSERINE externalization in a phospholipid bilayer at high transmembrane potential, J. Am. Chem. Soc. 128 (2006) 6288–6289.
[12] P.T. Vernier, Y. Sun, L. Marcu, C.M. Craft, M.A. Gundersen, Nano-electropulse-induced phosphatidylserine translocation, Biophys. J. 86 (2004) 4040–4048.
[13] Z. Levine, P.T. Vernier, Life cycle of an electropore: Field-dependent and field-independent steps in pore creation and annihilation, J. Membr. Biol. 236 (2010) 27–36.
[14] P.T. Vernier, Y. Sun, M.A. Gundersen, Nano-electropulse-driven membrane perturbation and small molecule permeabilization, BMC Cell Biol. 7 (2006) 37.
[15] A.G. Pakhomov, A.M. Bowman, B.L. Ibey, F.M. Andre, O.N. Pakhomova, K.H. Schoenbach, Lipid nanopores can form a stable, ion channel-like conduction pathway in cell membrane, Biochem. Biophys. Res. Commun. 385 (2009) 181–186.
[16] B.L. Ibey, D.G. Mixon, J.A. Payne, A. Bowman, K. Sickendick, G.J. Wilmink, W.P. Roach, A.G. Pakhomov, Plasma membrane permeabilization by 60- and 600-ns electric pulses is determined by the absorbed dose, Bioelectromagnetics 30 (2009) 92–99.
[17] A.G. Pakhomov, J. Kolb, R. Shevin, J. White, R.P. Joshi, K.S. Schoenbach, Long-lasting plasma membrane permeabilization in mammalian cells by nanosecond pulsed electric field, Bioelectromagnetics 28 (2007) 655–663.
[18] A.G. Pakhomov, O.N. Pakhomova, Nanopores: A distinct transmembrane passageway in electroporated cells, in: A.G. Pakhomov, D. Miklavcic, M.S. Markov (Eds.), Advanced Electroporation Techniques in Biology in Medicine, CRC Press, 2010.
[19] G.L. Craviso, S. Choe, P. Chatterjee, I. Chatterjee, P.T. Vernier, Nanosecond electric pulses: A novel stimulus for triggering Ca(2+) influx into chromaffin cells via voltage-gated Ca(2+) channels, Cell. Mol. Neurobiol. 30 (2010) 1259–1265.
[20] G.L. Craviso, P. Chatterjee, G. Maalouf, A. Cerjanic, J. Yoon, I. Chatterjee, P.T. Vernier, Nanosecond electric pulse-induced increase in intracellular calcium in adrenal chromaffin cells triggers calcium-dependent catecholamine release, IEEE Trans. Dielectr. Electr. Insul. 16 (2009) 1294–1301.
[21] E. Tekle, H. Oubrahim, S.M. Dzekunov, J.F. Kolb, K.H. Schoenbach, P.B. Chock, Selective field effects on intracellular vacuoles and vesicle membranes with nanosecond electric pulses, Biophys. J. 89 (2005) 274–284.
[22] W. Frey, J.A. White, R.O. Price, P.F. Blackmore, R.P. Joshi, R. Nuccitelli, S.J. Beebe, K.H. Schoenbach, J.F. Kolb, Plasma membrane voltage changes during nanosecond pulsed electric field exposure, Biophys. J. 90 (2006) 3608–3615.
[23] K.C. Smith, J.C. Weaver, Transmembrane molecular transport during versus after extremely large, nanosecond electric pulses, Biochem. Biophys. Res. Commun. 412 (1) (2011) 8–12.